RSC Advances

ROYAL SOCIETY OF CHEMISTRY

www.rsc.org/advances

Heparin-modified graphene oxide loading anti-cancer drug and growth factor with heat stability, long-term release property and lower cytotoxicity

Ting Wu[1], Bin Zhang[2], Yuanyuan Liang[3,4], Tao Liu[5,*], Jinyan Bu[1], Lixing Lin[1], Zhimin Wu[1], Hongxi Liu[1], Shuiping Wen[1], Shaozao Tan[2], Xiang Cai[1,*]

[1] Department of Light chemical engineering，Guangdong Polytechnic, Foshan 528041, P. R. China

[2] Department of Chemistry, Jinan University, Guangzhou 510632, P. R. China

[3] College of material chemistry and chemical Engineering, Hangzhou Normal University, Hangzhou 310036, P. R. China

[4] College of chemical and Biological Engineering, Zhejiang University, Hangzhou 310027, P. R. China

[5] Guangdong Center for Tuberculosis Control, Guangzhou 510630, P. R. China

Department of Otolaryngology, Zhujiang Hospital, Southern Medical University, Guangzhou, 510282, P. R. China

[*] Corresponding author. Tel/Fax: +86 0757 83106906. E-mail: taoliu18@126.com (T. Liu); cecaixiang@163.com (X. Cai).

Abstract

To realize the long-term release property of drug, reduce the cytotoxicity of anti-cancer drug and improve the heat stability of growth factor, a heparin-modified graphene oxide (Hep-GO) was prepared through a click reaction between azide-modified graphene oxide and propargylamine-modified heparin. Then, the Hep-GO was used as the carrier of doxorubicin hydrochloride (DOX) and granulocyte colony stimulating factor (G-CSF), and Hep-GO/DOX/G-CSF complex was fabricated. UV-Vis analysis was carried out to study the colloidal stability of Hep-GO in aqueous solution. Thermogravimetric test was used to determine its composition. Then, the loading process, *in vitro* release behavior, heat stability and cytotoxicity of Hep-GO/DOX/G-CSF complex were studied. The results showed that the Hep-GO/DOX/G-CSF complex displayed heat stability, long-term drug release property and lower drug cytotoxicity, suggesting the great potential application of Hep-GO as multifunctional drug delivery system.

Key words: graphene oxide; anti-cancer drug; growth factor; heat stability; cytotoxicity

1. Introduction

Doxorubicin hydrochloride (DOX) is a drug used in the treatments of a wide range of cancers, including hematological malignancies (blood cancers like leukaemia and lymphoma), many types of carcinoma (solid tumours) and soft tissue sarcomas. Common adverse effects of doxorubicin include nausea and vomiting (which are seen in roughly 30-90% of people treated with the drug), oral mucositis, oesophagitis, diarrhoea and skin reactions (including hand-foot syndrome) [1].

Chemotherapy can cause myelosuppression and unacceptably low levels of white blood cells, making patients susceptible to infections and sepsis. Granulocyte-colony stimulating factor (G-CSF) is a glycoprotein that stimulates the bone marrow to produce granulocytes and stem cells and release them into the bloodstream. In oncology and hematology, G-CSF is used with certain cancer patients to accelerate recovery from neutropenia after chemotherapy, allowing higher-intensity treatment regimens. But, the G-CSF easily loses the activity under room temperature [2].

Graphene oxide (GO), a special two-dimensional nanomaterial, has been widely investigated for its special physical properties and potential applications in nanoelectronic devices, transparent conductors and nanocomposite materials [3-5]. In recent years, a considerable amount of literatures have been reported for chemically modified GO as hydrophobic drug carrier, because its large plane can load many aromatic drugs through π-π stacking interaction. For example, Sun et al. synthesized a PEG-modified GO with good water dispersion for DOX delivery and cellular imaging [6,7]. Zhang et al. used folate-modified GO to load doxorubicin and camptothecin, and obtained a targeted drug

carrier for tumor [8]. Yang et al. prepared a GO/Fe_3O_4 hybrid nanoparticle for loading DOX to develop a potential controlled targeted drug carrier [9]. Bao et al. prepared chitosan-modified GO as a nanocarrier for drug and gene delivery, and showed a good result in HeLa cell [10].

Heparin is a biologically relevant and highly anionic polysaccharide, which has been widely studied due to its importance in medicine and biomedical applications, including its common clinical use as an anticoagulant [11]. In addition, heparin contains distinct recognition sites for growth factors, such as G-CSF [12] and other growth factors (bone morphogenetic protein, basic fibroblast growth factor, and transforming growth factor-β) [13-16].

In this paper, we attempted to prepare a drug/protein dual nanocarrier by modifying GO with heparin. The water-soluble heparin could not only functionalize GO for growth factors binding, but also enhance the stability of GO in aqueous solution. DOX and granulocyte colony stimulating factor (G-CSF) were used as model drugs for loading by heparin-modified GO, and their stability, long-term release property and cytotoxicity were studied.

2. Materials and methods

2.1 Materials

Graphene oxide (GO) was prepared by a two-step approach [17-19]. Heparin sodium salt (potency > 120 U/mg) was purchased from Qiyun Biological Technology Company in China. 3-Azidopropylamine was synthesized according to reported method [20]. 1-Ethyl-3-(3-dimethylaminopropyl) carbodiimide hydrochloride (EDC·HCl), N-hydroxy-

succinimide (NHS), 4-dimethylamiopryidine (DMAP), N,N-dicyclohexylcarbodiimide (DCC), sodium azide and propargylamine were purchased from Sigma-Aldrich and used without further purification. Doxorubicin hydrochloride (DOX) was obtained from BioBasic Inc., USA. Human granulocyte colony stimulating factor (G-CSF) was obtained from General Hospital of Guangzhou Military Command in China. Thiazolyl blue tetrazolium bromide (MTT) substance was purchased from Sigma-Aldrich (Shanghai, China). Mouse fibroblast cell line NIH-3T3 was supplied by General Hospital of Guangzhou Military Command. Human nasopharyngeal carcinoma CNE1 (CNE1) cells were supplied by General Hospital of Guangzhou Military Command. All other reagents were of analytical grade and were used without further purification.

2.2 Preparation of heparin-modified GO (Hep-GO)

Scheme 1

(1) Synthesis of azide-modified graphene oxide (GO-N_3)

For azide modification, 50 mg GO was dispersed in DMSO and sonicated for 30 min to obtain a homogenous dispersion. Then, 160 mg 3-azidopropylamine, 108 mg DCC and 31.35mg DMAP were added. After reaction for 48 h at room temperature, the solution was dialyzed (MWCO = 5 000) in distilled water for 3 d, and GO-N_3 was obtained after frozen to dry with a yield of 96%. FT-IR (KBr, cm^{-1}): 3430 (ν_{O-H}), 2920 (ν_{C-H}), 2100 ($\nu_{N=N-N}$), 1590 ($\nu_{C=O}$), 1410 (δ_{C-H}), 1250 (δ_{O-H}), 1110 ($\delta_{C=O}$) and 900-850 ($\delta_{=C-H}$). The content of azide group in GO-N_3 was analyzed by elemental analyzer (Vario EL, Elementar) and determined to be

2.59%.

(2) Synthesis of propargylamine-modified heparin (Hep-PA)

For propargylamine modification, 160 μL propargylamine, 448 mg EDC·HCl and 272 mg NHS was added into 10 mL heparin aqueous solution (80 mg/mL). Then, the pH value of the mixture was adjusted to 6.0-6.5. After reaction for 48 h at room temperature, the solution was dialyzed (MWCO = 5 000) for 3 d and frozen to dry to obtain Hep-PA (yield: 78%). ^{1}H NMR (300 MHz, D_2O): *d* (ppm) 2.68 (s, 1H, NHCH2CC*H*), 3.0 (m, 2H, NHCH_2CC*H*), 1.85 (s, 3H, OCH_3 of sugar units), 3.35-3.95 and 4.50 (m, 4H, backbone of sugar units). Based on the ^{1}H NMR analysis, 28 propargylamine molecules were found for each 100 sugar unit of heparin.

(3) Synthesis of heparin-modified graphene oxide (Hep-GO)

The synthesis route to heparin-modified graphene oxide (Hep-GO) was shown in scheme 1. Briefly, 10 mg GO-N_3 was dispersed in DMSO and sonicated for 30 min to obtain a homogenous dispersion. 5 mL Hep-PA solution (20 mg/mL), 12.5mg $CuSO_4 \cdot 5H_2O$ and 80mg sodium ascorbate were then added. Under atmospheric argon, the reaction was conducted at 40 ℃ for 24 h. The solution was dialyzed (MWCO = 14 000) for 3 d and frozen to dry. Hep-GO was then obtained with a yield of 72%. Its structure was characterized by ^{1}H NMR analysis with the help of a 300 MHz Bruker Avance DPX-300 spectrometer (using D_2O as solvent), and FTIR analysis with the help of a Nicolet 670 Fourier-transform infrared spectrometer (using KBr pellets). The composition of Hep-GO was analyzed by Thermogravimetric (TG) test with a temperature range of 50-600 ℃ and a scan rate of 10 ℃/min. And its dispersion stability in aqueous solution was studied using a UV-Vis

spectrophotometer at an absorbance wavelength of 500 nm.

2.3 Loads of DOX and G-CSF

Doxorubicin hydrochloride (DOX) was dissolved in water with the concentration of 10 mg/mL, and Hep-GO was dispersed in aqueous solutions with the concentration of 10 mg/mL. Then, DOX solution (1 mL) was added into Hep-GO dispersion (1 mL) drop by drop. The resultant mixture was stirring at room temperature for 24 h, and then centrifugated at 50 000 r/min for 10 min. After washing with distilled water for three times, the residue was frozen to dry to obtain the DOX-loaded Hep-GO (Hep-GO/DOX). The loading efficiency of DOX on Hep-GO was calculated by analyzing centrifugation solution using UV-Vis spectrophotometer at the absorbance wavelength of 480 nm [21].

To obtain the Hep-GO/G-CSF or Hep-GO/DOX/G-CSF complex, 1 mL Hep-GO or Hep-GO/DOX mixture (Hep-GO: 10 mg/mL) was mixed with 1 mL G-CSF solution (10 mg/mL). The resultant mixture was stirring at room temperature for 30 min, and then dialyzed (MWCO = 30 000) for 24 h with distilled water to remove free G-CSF. The loading efficiency of G-CSF was analyzed by ELISA assay.

In Hep-GO/DOX, 712 mg DOX was loaded onto 1 g Hep-GO; in Hep-GO/G-CSF, 967 mg G-CSF was loaded onto 1 g Hep-GO; in Hep-GO/DOX/G-CSF, 687 mg DOX and 933 mg G-CSF were loaded onto 1 g Hep-GO.

The zeta potentials and particle sizes of Hep-GO, Hep-GO/DOX and Hep-GO/DOX/G-CSF were studied by a Zeta Potential Analyzer instrument (ZetaPALS, Brookhaven Instruments Corporation, USA). TEM test was used to observe their morphologies.

2.4. *In vitro* release

The simulated gastrointestinal medium and the amount of Hep-GO/DOX/G-CSF that was added were determined from previous reports [22,23]. Briefly, the simulated gastric fluid was a solution of 0.1 mol/L hydrochloric acid (pH=1.2), and 140 mg of the Hep-GO/DOX/G-CSF was added to 10 mL of the simulated stomach fluid. The simulated small intestinal fluid was prepared with pH=6.8 PBS containing 1% of pancreatin, and 95 mg of Hep-GO/DOX/G-CSF was added to 10 mL of the simulated small intestine medium. The simulated colon fluid was prepared as a pH=7.2 buffer medium that was composed of 0.15 wt% potassium dihydrogen orthophosphate, 0.15 wt% dipotassium hydrogen orthophosphate, 0.45 wt% sodium chloride, 0.05 wt% magnesium chloride hexahydrate, 0.005 wt% ferrous sulphate heptahydrate, 0.015 wt% calcium chloride dihydrate and 0.015 wt% sufficient sodium hydroxide, and 1 g of Hep-GO/DOX/G-CSF was added to 10 mL of the simulated colon medium.

The release studies were conducted at 37 °C under slow stirring (50 rpm). The supernatant (2.0 mL) was withdrawn periodically at predetermined time interval, and another 2.0 mL of simulated gastrointestinal medium was added to continue the experiment. The supernatant was dialysed (immersed in PBS (pH=7.4) with a dialysis bag, molecular weight cut off of 3000). The amount of released DOX was determined according to a method reported previously by a UV pectrophotometer (S52, China) at the absorbance wavelength of 480 nm [20], and G-CSF was determined by ELISA assay. The percentage of cumulative amount of released drug was calculated from standard calibration curve. All release studies were carried out in triplicate.

2.5 Heat stability

262 mg Hep-GO/DOX/G-CSF (containing 100 mg Hep-GO, 68.7 mg DOX and 93.3 mg G-CSF) or 93.3 mg G-CSF was respectively immersed in 50 mL pH=7.0 ultrapure water at 25 ℃, 35 ℃, 45 ℃ or 60 ℃. At predetermined time point, the solution was cooled to 25 ℃, and then centrifugated at 50 000 r/min for 10 min. After that, the concentration of DOX was calculated by analyzing centrifugation solution using UV-Vis spectrophotometer at the absorbance wavelength of 480 nm [21].

2.6 Cytotoxicity assay.

Cytotoxicity of sample was tested using the MTT assay based on the cellular uptake of MTT and its subsequent reduction in the mitochondria of living cells to dark blue MTT formazan crystals. NIH-3T3 cells or CNE1 cells were seeded on 96-well plates ($1.5\text{-}2\times10^4$ cells/well) in corresponding medium. Then, the NIH-3T3 cells or CNE1 cells were treated with the samples for 24 h. After that, MTT (5 mg/mL in PBS) was added to each well and incubated for additional 4 h (37 ℃, 5% CO_2). The cells were then lyzed in dimethyl sulfoxide (150 μL/well) and the plates were allowed to stay in the incubator (37 ℃, 5% CO_2) to dissolve the purple formazan crystals. The color intensity reflecting cell viability was read at 490 nm using a Model-550 Enzyme-linked immunosorbent microplate (Bio-Rad, USA), and the morphologic changes of NIH-3T3 cells or CNE1 cells were photographed by a IX-70 inverted phase contrast microscope (Olympus, Japan). All the experiments were repeated four times and Statistical Product and Service Solutions software was used to assess statistical significance of the differences among treatment groups.

2.7 Statistical analysis

The statistical analysis was performed using Statistical Product and Service Solutions statistical software (SPSS 11.0, United States). The differences between the groups were assessed using the analysis of variance test. The results were considered statistically significant when the P value was <0.05 or <0.01.

3. Results and discussion

Figure 1

Figure 1(A) showed the ^{1}H NMR spectra of Hep-PA and Hep-GO. Compared with that of Hep-PA, the spectrum of Hep-GO showed a new peak at 7.80 ppm, which could be contributed to the presence of the triazole proton due to Cu(I)-catalyzed Huisgen 1,3-dipolar cycloaddition of GO-N_3 with Hep-alkynyl. Such a signal was also observed by Srinivasachari *et al*. [24] who synthesized multivalent polycationic β-cyclodextrin "click clusters" by reacting an acetylated-per-azido-β-cyclodextrin with the alkyne dendrons containing one to five ethyleneamine units with the help of copper-catalyzed 1,3-dipolar cycloaddition. Besides, another new peak at 2.59 ppm might be attributed to the methylene protons from 3-azidopropylamin of GO-N_3. To further confirm the chemical structure of Hep-GO, FT-IR test was carried out and the result was showed in Figure 1(B). Before click-reaction, Hep-PA and GO-N_3 showed their characteristic absorption bands, respectively. Particularly, GO-N_3 sample showed the obvious band of azido group at 2100 cm^{-1} [25]. After the click conjugation, the spectrum of the resultant Hep-GO did not show the characteristic absorption band of the azido at 2100 cm^{-1}. However, it exhibited the main characteristic absorption

bands of Hep-PA and GO-N_3, which confirmed the click conjugation reaction and all azido groups of GO-N_3 reacted with Hep-PA.

The composition of the obtained Hep-GO was analyzed by TG test shown in Figure 1(C). Under nitrogen atmosphere, GO-N_3 sample remained about 65.87% residue after heated to 600 °C, while Hep-PA sample only remained 30.79%. Hep-GO sample began to decompose at about 240 °C and remained 39.65% residue. From these results, the content of heparin in Hep-GO could be calculated to be 74.7 wt%.

Figure 2

Figure 2 showed the colloidal stability characterization of Hep-GO in aqueous solution. Figure 2(A) gave the change of relative absorbance with respect to the setting time for GO and Hep-GO samples. It was found that there was little change in relative absorbance for Hep-GO sample after 12 h, which proved that the obtained Hep-GO dispersion had a good colloidal stability. As a contrast, the pure GO without modification by heparin showed a faster deposition in aqueous solution. Inset image showed the typical results of Hep-GO and GO aqueous samples after 4 d. In order to confirm the homogenous dispersion of the Hep-GO in aqueous solution, UV-Vis absorption spectra were collected for different Hep-GO concentrations. As shown in Figure 2(B), the intensities of absorption spectra had a good linear relation with the concentrations of Hep-GO (inset figure), i.e., following Lambert-Beer's law. This result confirmed that Hep-GO showed a good dispersion in aqueous solution [26]. From these results, it seemed that the utilization of heparin could function as an effective stabilizing agent for the formation of colloidal stable Hep-GO sample.

In fact, the obtained colloidal Hep-GO showed a macroscopically homogeneous dispersion more than two weeks.

Figure 3

Due to the interactions between heparin and growth factors, meanwhile between GO and drugs, Hep-GO could be used as dual carrier for drug and protein. Figure 3(A) showed the particle size and zeta potential results of Hep-GO, Hep-GO/DOX and Hep-GO/DOX/G-CSF. GO showed a zeta potential of -21.23 mV and particle size of 907 nm. Due to the carboxyl groups of GO plane sheet and electronegative groups of heparin, Hep-GO showed a zeta potential of -29.36 mV and particle size of 817 nm. After loading DOX onto GO sheet, the Hep-GO/DOX complex showed a decreased zeta potential of -22.04 mV and particle size of 634 nm, respectively. This result might be due to the interaction between electropositive DOX and Hep-GO, which resulted in a slight shrinkage of Hep-GO nanoparticles. After binding G-CSF followed, the obtained Hep-GO/DOX/G-CSF showed a further smaller particle size (568.8 nm) but an increased zeta potential (-23.22 mV), which might be caused due to the net negative charge of G-CSF. Figure 3(B) showed the TEM images of Hep-GO, Hep-GO/DOX and Hep-GO/DOX/G-CSF. It could be seen that all samples in these cases showed the nanosheet morphologies with good dispersion in aqueous solution.

Figure 4

The average residence time for a dosage form in the gastrointestinal system was different after oral administration, which was approximately 1-3 h in the stomach, 3-5 h in

the small intestine, and 30-50 h in the colon [22, 23]. The *in vitro* DOX and G-CSF release behaviours of the Hep-GO/DOX/G-CSF were evaluated in different simulated gastrointestinal media (Figure 4). To overcome the undesirable side effects of DOX and G-CSF after oral administration, the Hep-GO/DOX/G-CSF must sustain the releases of the DOX and G-CSF. As shown in Figure 4, various release rates were found. In all the cases, the releases of DOX and G-CSF could be prolonged and no initial burst release was obvious, which indicated that the releases of DOX and G-CSF could be controlled and sustained in the Hep-GO/DOX/G-CSF form. These results indicated that the Hep-GO/DOX/G-CSF was stable in simulated gastric fluid, and it reduced the undesirable side effect of DOX. Sustained release and high DOX or G-CSF cumulative release were achieved in the Hep-GO/DOX/G-CSF, which was important in drug delivery.

To understand the DOX and G-CSF release mechanisms of Hep-GO/DOX/G-CSF, we fitted the accumulative release data using the semiempirical equation (5) [27, 28]:

$$M_t / M_\infty = Kt^n \quad \left(for\ M_t / M_\infty \le 0.6\right) \qquad (5)$$

Where M_t and M_∞ were respectively the cumulative amount of the drug released at t and equilibrium, K was the rate constant relating to the properties of the hydrogel matrix and the drug, and n was the release exponent characterising the transport mechanism.

By plotting log (M_t/M_∞) versus log (t), the n values as well as the corresponding determination coefficients (R^2) were obtained. The n values were between 0.53 and 0.72, and the R^2 values were greater than 0.98. According to the semi-empirical equation (5), there were four distinguishable modes of diffusion, as follows: (i) the value of n=0.5 suggested Fickian or Case I transport behaviour, in which the relaxation coefficient was negligible

during transient sorption; (ii) the value of n=1 referred to a non-Fickian or Case II mode of transport in which the morphological change was abrupt; (iii) if $0.5<n<1$, the transport process was anomalous, corresponding to Case III, and the structural relaxation was comparable to diffusion; (iv) a value of $n<0.5$ indicated a pseudo-Fickian diffusion behaviour, in which the sorption curve resembled Fickian curve, with the speed of the approach to the final equilibrium being very slow. In our case, the n values were found to be in the 0.5 to 1 range, showing a Case III mechanism, which indicated that the structural relaxation was comparable to diffusion (Table 1).

Table 1

The *in vitro* evaluation suggested that the Hep-GO/DOX/G-CSF exhibited sustained release behaviour in the simulated medium of the gastrointestinal tract. This finding might be helpful for decreasing damage of DOX to the gastrointestinal tract and achieving long-term and sustained releases of DOX and G-CSF for efficient clinical use [29,30].

Figure 5

As shown in figure 5, a rise in temperature would accelerate the rate of degradation of G-CSF. With the rise in temperature, the rate of degradation of G-CSF was accelerated. But, the G-CSF in Hep-GO/G-CSF was more stable in heating condition than the G-CSF alone. Since the Hep-GO bundled the G-CSF, the G-CSF in Hep-GO/G-CSF would be isolated from heating condition, which made the G-CSF more stable than the G-CSF alone and would

extend the store and application condition of G-CSF.

Figure 6

The cytotoxicity test on the sample was also carried out. As shown in Figure 6(A), G-CSF acted as a growth hormone promoting NIH-3T3 cellular growth and preventing apoptosis. Hep-GO (100 μg/mL) exhibited a slight cytotoxicity (15.7%) to NIH-3T3 within 24 h incubation. DOX exhibited a serious cytotoxicity to NIH-3T3 within 24 h incubation (the cell viability of NIH-3T3 was reduced to 6.0% with 100 μg/mL DOX). However, the cell viability of NIH-3T3 was reduced to 35.0% with 100 μg/mL DOX-loaded Hep-GO/DOX, while the cell viability of NIH-3T3 was reduced to 45.0% with 100 μg/mL DOX-loaded Hep-GO/DOX/G-CSF, since there was G-CSF in Hep-GO/DOX/G-CSF. Therefore, the cytotoxicity of Hep-GO/DOX/G-CSF was significantly lower than DOX, and the use of DOX would be safer than the direct use of DOX, which was in accordance with the results of inverted phase contrast microscope measurements (Figure 6(B)). In Figure 6(B), when the concentrations of total DOX and G-CSF in samples were set at 100 μg/mL, the NIH-3T3 cells showed different morphologic changes after interaction for 24 h: In the blank control group (a), the NIH-3T3 cells had good shape and presented long fusiform or polygon. In the GO group (b) (100 μg/mL), the NIH-3T3 cells decreased slightly, but the NIH-3T3 cells still had good shape and presented long fusiform or polygon. In the Hep-GO group (c), the NIH-3T3 cells also decreased slightly, but the NIH-3T3 cells still had good shape and presented long fusiform or polygon. In the DOX group (d), the number of NIH-3T3 cells

decreased significantly, and the shapes of majority of the cells were seriously injured. In the G-CSF group (e), the NIH-3T3 cells had better shape. In the Hep-GO/DOX group (f), the number of NIH-3T3 cells decreased, and the shapes of majority of the cells were seriously injured. In the Hep-GO/DOX/G-CSF group (g), the number of NIH-3T3 cells decreased, but the shapes of the cells still presented long fusiform or polygon. Compared with other reports [17-19], we concluded that Hep-GO/DOX/G-CSF was relatively biocompatible nanomaterial with reduced cytotoxicity.

Figure 7

As shown in Figure 7(A), DOX exhibited a serious cytotoxicity to CNE1 within 24 h incubation (the cell viability of NIH-3T3 was reduced to 4.1% with 500 μg/mL DOX). However, the cell viability of CNE1 was reduced to 9.1% with 500 μg/mL DOX-loaded Hep-GO/DOX, while the cell viability of CNE1 was reduced to 9.7% with 500 μg/mL DOX-loaded Hep-GO/DOX/G-CSF. Therefore, the cytotoxicity of Hep-GO/DOX/G-CSF on CNE1 cells was as much the same as DOX, but the use of Hep-GO/DOX/G-CSF would be safer than the direct use of DOX, which was in accordance with the results of inverted phase contrast microscope measurements (Figure 6(B)). In Figure 6(B), when the concentrations of total DOX in samples were set at 100 μg/mL, the CNE1 cells showed different morphologic changes after interaction for 24 h: In the blank control group (a), the CNE1 cells had good shape and presented long fusiform or polygon. In the DOX group (b), the Hep-GO/DOX group (c) and the Hep-GO/DOX/G-CSF group (g), the number of CNE1 cells decreased

significantly, and the shapes of majority of the cells were seriously injured.

The *in vitro* release characterization indicated that both of two model drugs showed a long-term drug release property, heat stability and lower drug cytotoxicity. The π-π bonding interaction and ionic bond interaction between carrier (Hep-GO) and drugs (DOX and G-CSF) was controlled the drug load and long-term drug release property [17-19]. What is more, the long-term DOX release, along with the coating of DOX into Hep-GO also reduced the cytotoxicity of DOX. Since the G-CSF will be exposed to environmental conditions different from a research lab setting, many factors, including light, temperature, salinity, etc., are suspected to affect the stability of the G-CSF [2]. The Hep-GO anchored the G-CSF and isolated the G-CSF from outside, thus G-CSF in Hep-GO/DOX/G-CSF showed heat stability.

Compared with other reports [13-16], we concluded that the carrier of Hep-GO has better biocompatible, and exhibited a great potential as multifunctional drug delivery nanocarrier.

Conclusion

A dual drug nanocarrier had been prepared by the click conjugation of heparin with graphene oxide. The model drugs, doxorubicin hydrochloride (DOX) and granulocyte colony stimulating factor (G-CSF), were then loaded. UV-Vis analysis confirmed that this Hep-GO had high loading efficiencies for DOX and G-CSF. The *in vitro* release characterization indicated that both of two model drugs showed a long-term drug release property, better heat stability and lower drug cytotoxicity. Such a Hep-GO exhibited a great potential as multifunctional drug delivery nanocarrier.

Acknowledgements

The authors acknowledge financial support from the National Natural Science Foundation of China (51172099, 51203134, 21476052 and 21271087), the Foundation of Enterprise-University- Research Institute Cooperation from Guangdong Province and the Ministry of Education of China (2013B090600148), the Natural Science Foundation of Guangdong Province (2015A030313864), and The Science and Technology Innovation Platform Project of Foshan City (2014AG100171).

Author contributions

Ting Wu and Jinyan Bu prepared heparin-modified graphene oxide; Bin Zhang and Lixing Lin loaded anti-cancer drug and growth factor onto heparin-modified graphene oxide; Yuanyuan Liang and Zhimin Wu characterized the complex; Ting Wu, Hongxi Liu, and Shuiping Wen conducted *in vitro* evaluation; Ting Wu, Bin Zhang, Shaozao Tan and Xiang Cai analysed the data and wrote the manuscript; Shaozao Tan and Xiang Cai conceived of this project, designed the experiments; all authors discussed the results and commented on the manuscript.

References

[1] O. Tacar, P. Sriamornsak, C. R. Dass, J. Pharm. Pharmacol. 2014. 65. 157.

[2] H. S. Lu, C. L. Clogston, L. O. Narhi, L. A. Merewether, W. R. Pearl, T. C. Boone, J. Biol. Chem. 1992. 267. 87701.

[3] V. Singh, D. Joung, L. Zhai, S. Das, S. I. Khondaker, S. Seal, Prog. Mater. Sci. 2011. 56. 1178.

[4] V. C. Sanchez, A. Jachak, R. H. Hurt, A. B. Kane, Chem. Res. Toxicol. 2012. 25. 15.

[5] Huang, X.; Qi, X.; Boeya, F.; Zhang, H. Graphene-based composites. Chem. Soc. Rev. 2012. 41. 666.

[6] Z. Liu, J. T. Robinson, X. Sun, H. Dai, J. Am. Chem. Soc. 2008. 130. 10876.

[7] X. Sun, Z. Liu, K. Welsher, J. T. Robinson, A. Goodwin, S. Zaric, H. Dai, Nano. Res. 2008. 1. 203.

[8] L. Zhang, J. Xia, Q. Zhao, L. Liu, Z. Zhang, Small 2010. 6. 537.

[9] X. Y. Yang, X. Y. Zhang, Y. F. Ma, Y. Huang, Y. S. Wang, Y. S. Chen, J. Mater. Chem. 2009. 19. 2710.

[10] H. Bao, Y. Pan, Y. Ping, N. G. Sahoo, T. Wu, L. Li, J. Li, L. H. Gan, Small 2011. 7. 1569.

[11] F. J. Spinelli, K. L. Kiick, E. M. Furst, Biomaterials 2008. 29. 1299.

[12] H. Layman, M. Sacasa, A. E. Murphy, A. M. Murphy, S. M. Pham, F. M. Andreopoulos, Acta Biomater. 2009. 5. 230.

[13] L. Bromberg, J. Control. Release 2008. 128. 99.

[14] Y. Chung, K. M. Ahn, S. H. Jeon, S. Y. Lee, J. H. Lee, G. Tae, J. Control. Release 2007. 121. 91.

[15] Y. C. Ho, F. L. Mia, H. W. Sung, P. L. Kuo, Int. J. Pharmaceut. 2009. 376. 69.

[16] J. S. Lee, D. H. Go, J. W. Bae, S. J. Lee, K. D. Park, J. Control. Release 2007. 117. 204.

[17] X. Cai, S. Tan, A. Yu, J. Zhang, J. Liu, W. Mai, Z. Jiang, Chem-Asian J. 2012. 7. 1664.

[18] X. Cai, M. Lin, S. Tan, W. Mai, Y. Zhang, Z. Liang, Z. Lin, X. Zhang, Carbon 2012. 50. 3407.

[19] X. Cai, S. Tan, M. Lin, A. Xie, W. Mai, X. Zhang, Z. Lin, T. Wu, Y. Liu, Langmuir 2011. 27. 7828.

[20] X. Jiang, J. Zhang, Y. Zhou, J. Xu, S. Liu, J. Polym. Sci. Pol. Chem. 2008. 46. 860.

[21] X. Yang, X. Zhang, Z. Liu, Y. Ma, Y. Huang, Y. Chen, J. Phys. Chem. C. 2008. 112. 17554.

[22] X. Cai, L. Q. Yang, L. M. Zhang, Q. Wu, Carbohyd. Res. 2010. 345. 922.

[23] X. Cai, L. Q. Yang, L. M. Zhang, Q. Wu, Bioresource. Technol. 2009. 100. 4164.

[24] S. Srinivasachari, K. M. Fichter, T. M. Reineke, J. Am. Chem. Soc. 2008, 130, 4618,

[25] J. Xu, S. Liu, J. Polym. Sci. Pol. Chem. 2009. 47. 404.

[26] Z. Wang, Q. Liu, H. Zhu, H. Liu, Y. Chen, M. Yang, Carbon 2007. 45. 285.

[27] D. Ma, Z. Liu, Q. Zheng, X. Zhou, Y. Zhang, Y. Shi, J. Lin, W. Xue, Macromol. Rapid Comm. 2013. 34. 548.

[28] D. Ma, K. Tu, L. Zhang, Biomacromolecules 2010. 11. 2204.

[29] D. Ma, Q. Lin, L. Zhang, Y. Liang, W. Xue, Biomaterials 2014. 35. 4357.

[30] T. Liu, W. Xue, B. Ke, M. Q. Xie, D. Ma, Biomaterials 2014. 35. 3865.

Table 1. The kinetics parameters of DOX and G-CSF releases.

simulated medium	Drug	K^*	n^{**}	R^2	Transport mechanism
stomach fluid	DOX	0.78 ± 0.07	0.51 ± 0.05	0.95	Case III
	G-CSF	0.56 ± 0.01	0.57 ± 0.01	0.99	Case III
small intestine	DOX	0.82 ± 0.03	0.49 ± 0.03	0.98	Case III
	G-CSF	0.57 ± 0.02	0.55 ± 0.04	0.94	Case III
colon	DOX	0.83 ± 0.04	0.46 ± 0.02	0.96	Case III
	G-CSF	0.62 ± 0.04	0.54 ± 0.03	0.95	Case III

* K, rate constant, ±SD, n = 3.

** n, release exponent, ±SD, n = 3.

Figure cpture:

Scheme 1. Step 1, synthesis route to azide-modified graphene oxide (GO-N_3); step 2, synthesis route to propargylamine-modified heparin (Hep-PA); step 3, synthesis route to heparin-modified graphene oxide (Hep-GO).

Figure 1. (A) 1H NMR spectra of Hep-PA and Hep-GO (D_2O, 25 ° C). (B) FT-IR spectra of Hep-PA, GO-N_3 and Hep-GO. (C) TG curves of Hep-PA, GO-N_3 and Hep-GO.

Figure 2. (A) The changes of relative absorbance with respect to the setting time for GO and Hep-GO in aqueous solution at 500 nm (inset was the picture of Hep-GO and GO aqueous dispersion after 4 d). (B) UV-vis absorption spectra of Hep-GO in water with different relative concentrations of C_0 (C_0 denoted the original concentration of Hep-GO in water; 1: $1.0C_0$, 2: $0.8C_0$, 3: $0.6C_0$, 4: $0.4C_0$, 5: $0.2C_0$). Inset was Lambert-Beer's plot for the absorption at 500 nm.

Figure 3. (A) Particle size and (B) zeta potential results of GO, Hep-GO, Hep-GO/DOX and Hep-GO/DOX/G-CSF. (C) TEM images of GO, Hep-GO, Hep-GO/DOX and Hep-GO/DOX/G-CSF.

Figure 4. The release behaviours of DOX and G-CSF from the Hep-GO/DOX/G-CSF in the simulated medium of the gastrointestinal tract (±SD, $n = 3$).

Figure 5. Stabilities of G-CSF and Hep-GO/G-CSF preserved in different pH aqueous solution at various temperatures.

Figure 6. (A) Cytotoxicity of sample on NIH-3T3 cells. (B) When the concentrations of the samples were set at 100 μg/mL, the morphologic changes of NIH-3T3 cells after interaction for 24 h. (In Hep-GO/DOX and Hep-GO/DOX/G-CSF, the concentration meant the total DOX in sample).

Figure 7. (A) Cytotoxicity of sample on CNE1 cells. (B) When the concentrations of the samples were set at 100 μg/mL, the morphologic changes of CNE1 cells after interaction for 24 h. (In Hep-GO/DOX and Hep-GO/DOX/G-CSF, the concentration meant the total DOX in sample).

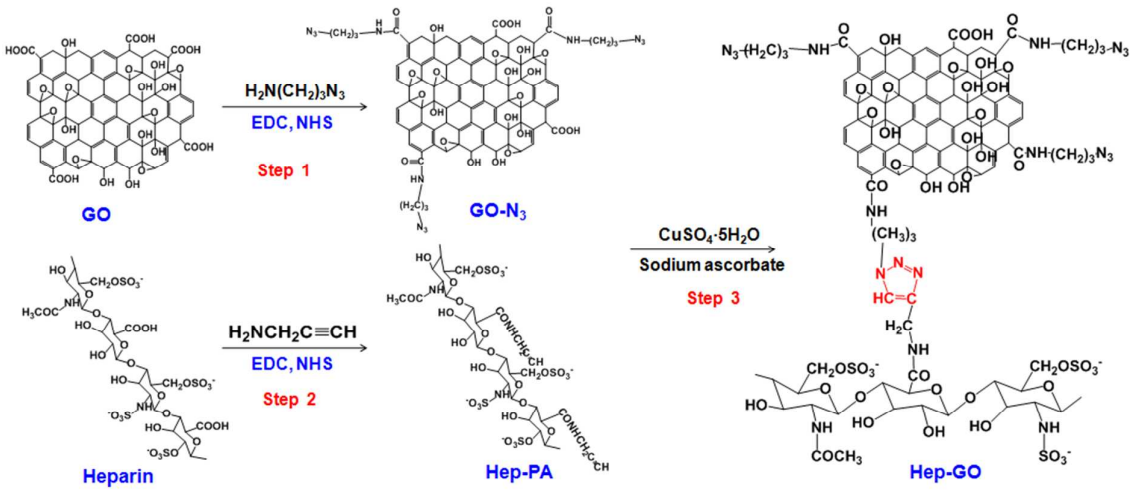

Scheme 1

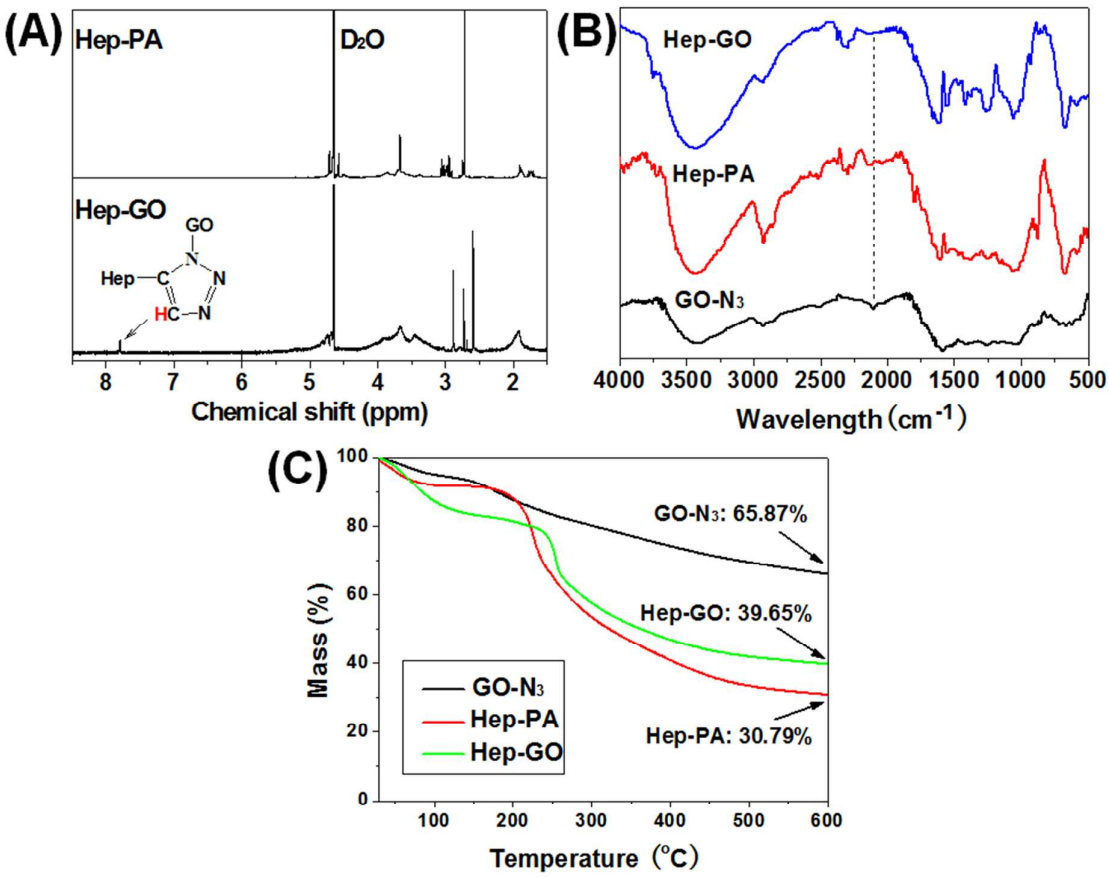

Figure 1

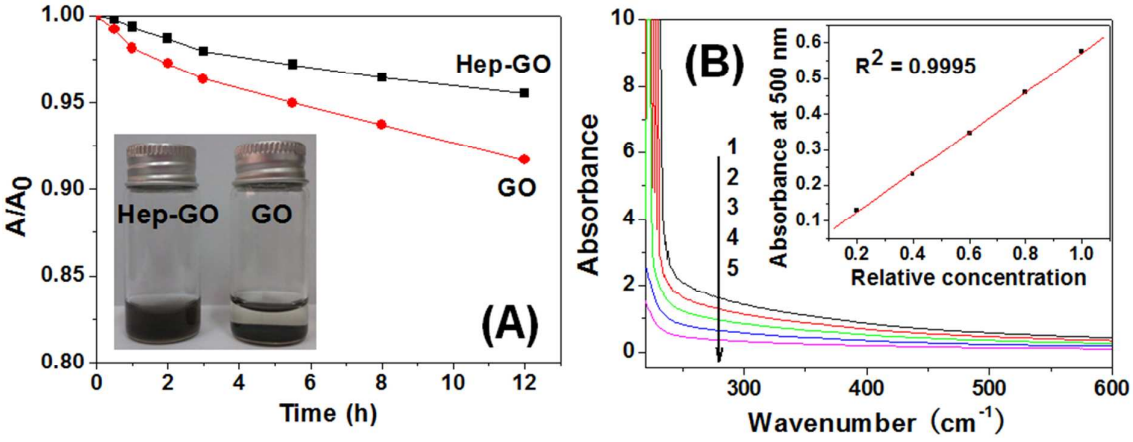

Figure 2

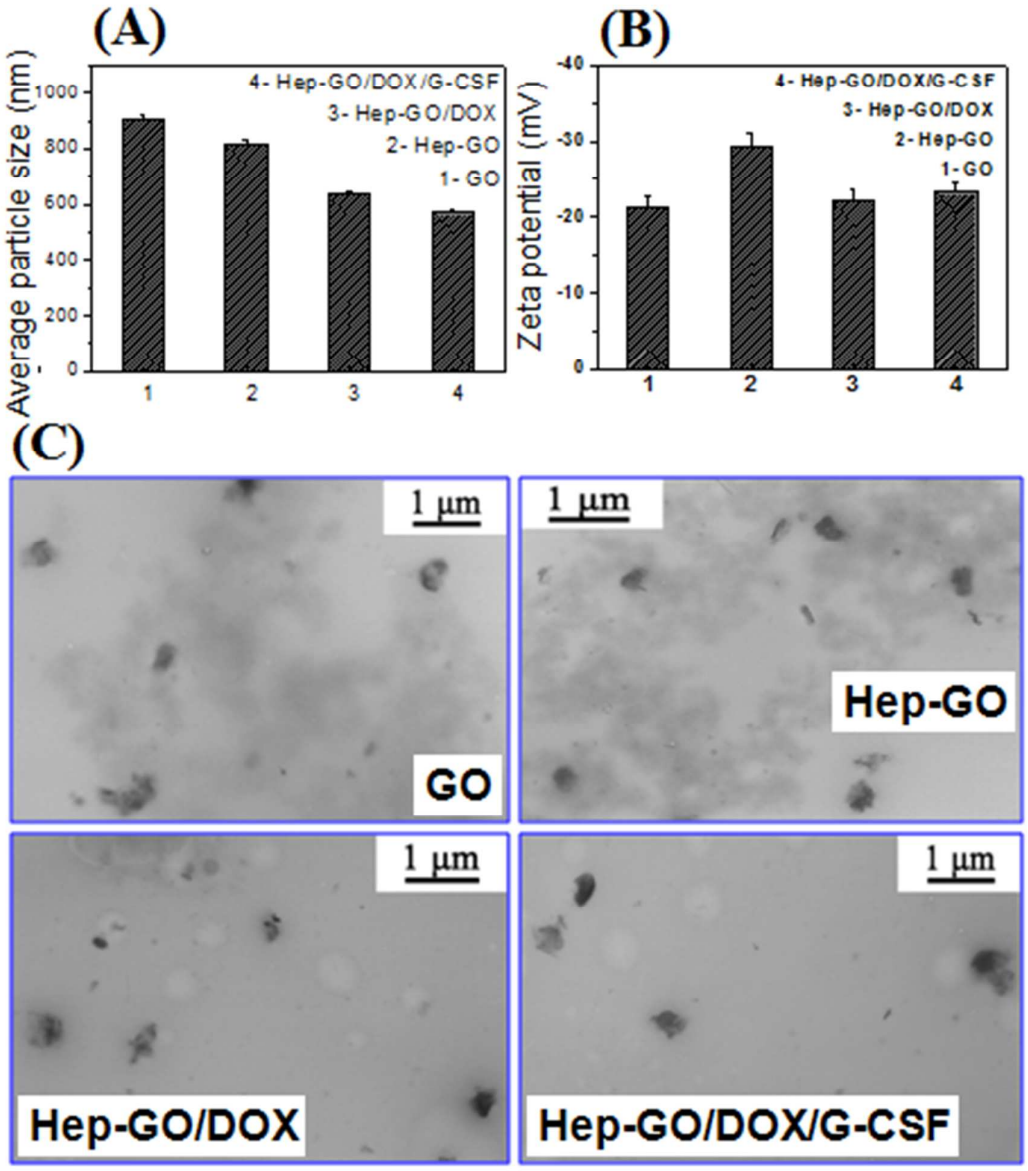

Figure 3

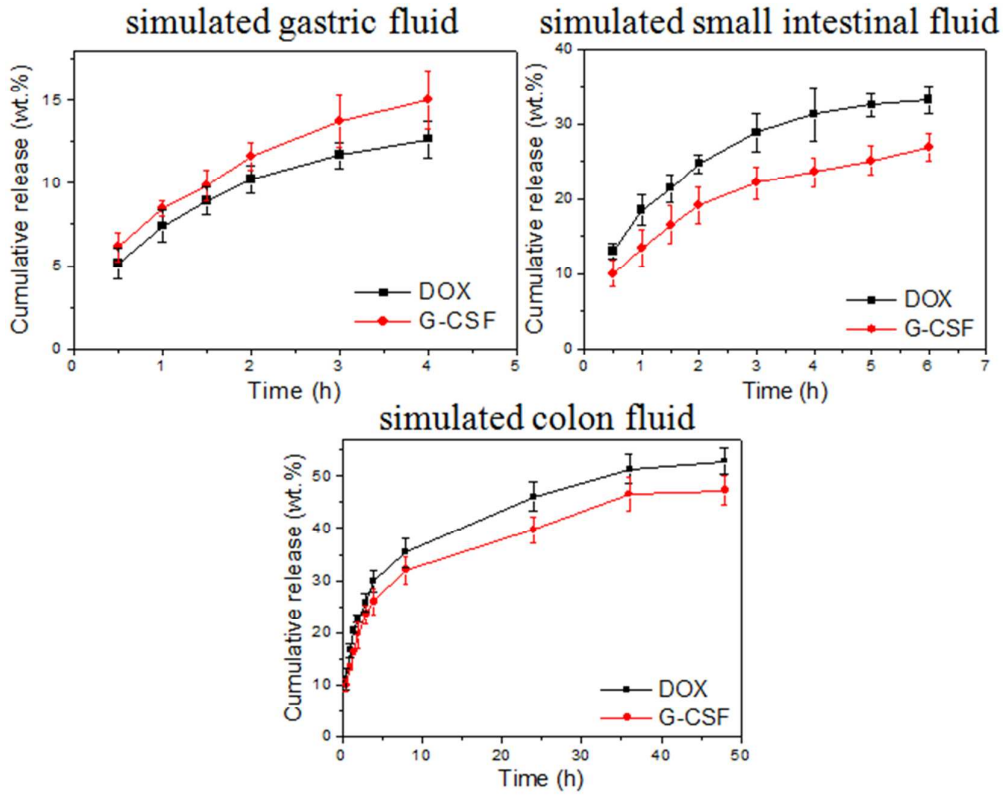

Figure 4

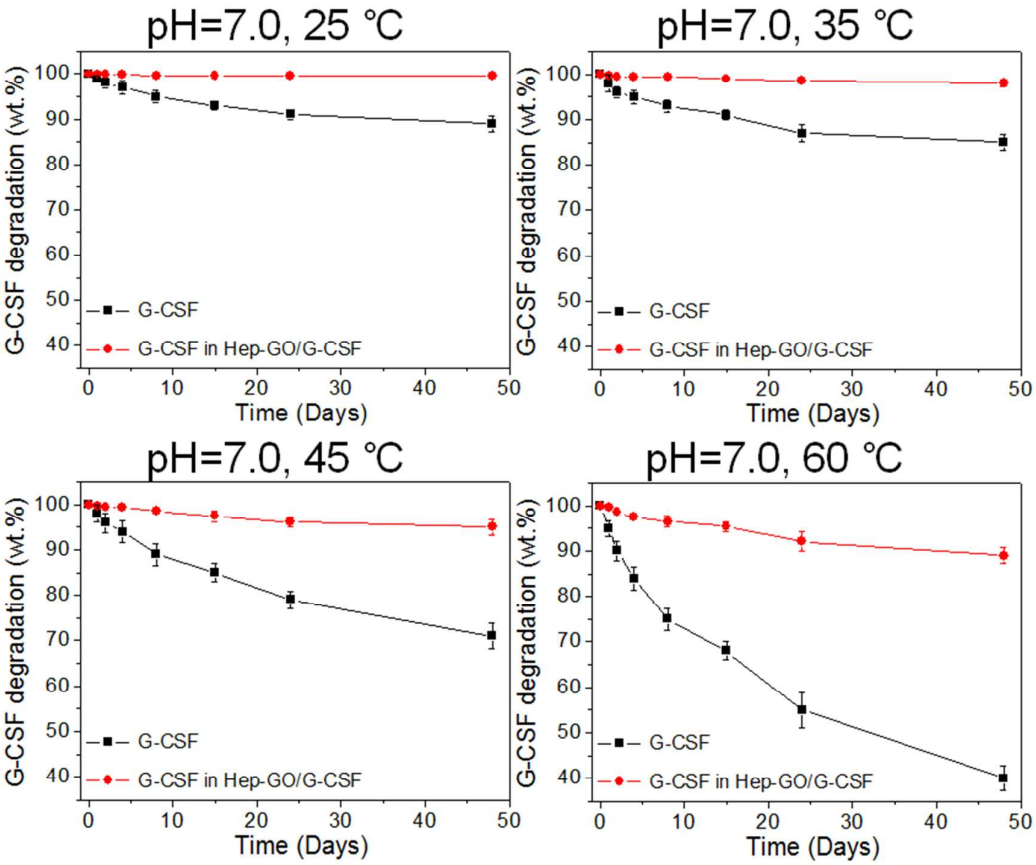

Figure 5

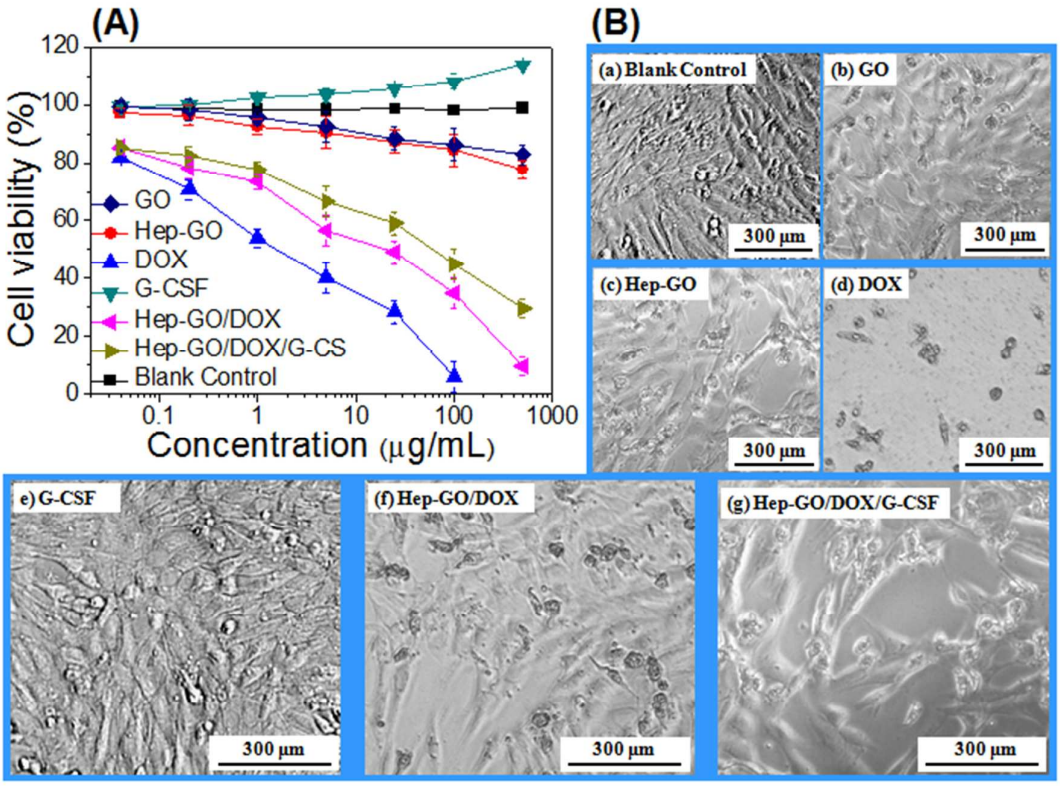

Figure 6

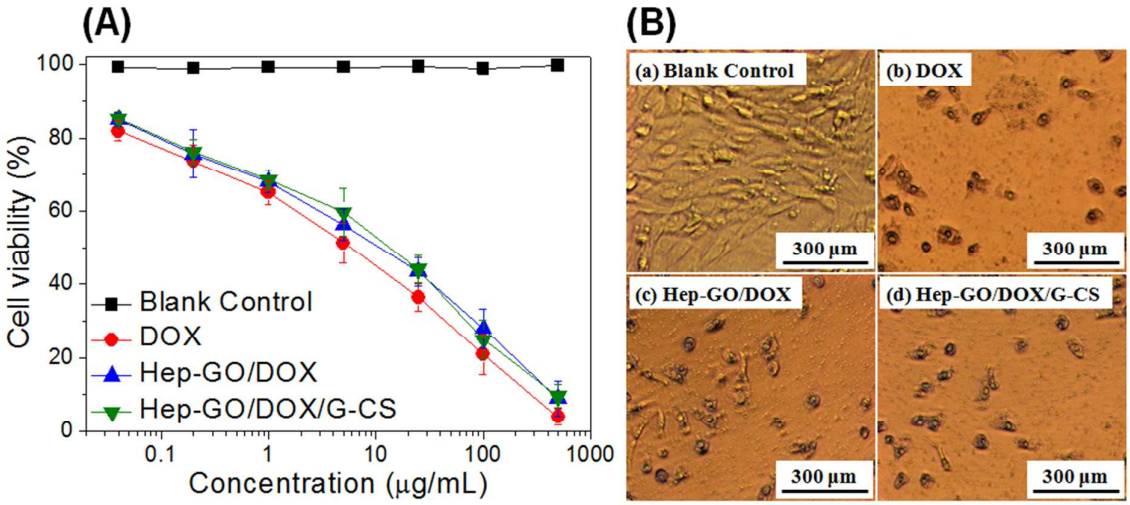

Figure 7